Reducing Emissions of Atmospheric Pollutants along Major Dry Bulk and Tanker Routes through Autonomous Shipping

Jiahui Liu, Adrian Wing-Keung Law*, and Okan Duru

School of Civil and Environmental Engineering, Nanyang Technological University, 50 Nanyang Avenue, Singapore 639798

*Corresponding author: cwklaw@ntu.edu.sg

Abstract

The present study investigates the environmental benefits of phasing-in autonomous ships in global maritime transportation along major dry bulk and tanker routes using Bayesian probabilistic forecasting algorithm. The focus is on the simulations and calibrations on the navigational behavior of autonomous ships at both port and high-sea, as well as the potential emission abatement of atmospheric pollutants compared to the conventional fleet along the sailing routes. We use historical data on major international tanker and dry bulk trade routes to characterize the ship movements and trends in ship emission. Different scenarios are evaluated with a combination of autonomous ship phase-in rates (25, 75, 100%) and cleaner fuel choices in Years 2030 and 2050 (from the baseline Year 2020). The results show that the magnitude of the emission reduction generally increases with a higher level of autonomous ships in the fleet as expected, and the magnitude ranges from small increments to major reductions of 37-64% along the different routes. Overall, we hope that our findings can contribute towards the realization of environmental benefits with the adoption of autonomous shipping along the major shipping routes in the future.

Keywords: autonomous shipping; emission; Bayesian forecasting; port-to-port optimization.

1. Introduction

The advancement of Maritime Autonomous Surface Ships (MASS) is progressing rapidly with their potentials to enhance navigation, efficiency, and environmental protection. Their practical adoption into the maritime fleet can occur as coastal vessels from as early as the first half of Year 2020s, and as commercial cargo ships by Year 2035 (Rødseth Ørnulf, 2013; Rolls-Royce, 2016a). The disruption can transform existing practices in the logistic chain and redefine the maritime industry in numerous ways, including: 1) the port can better integrate the transport system and facilitate port entries and ship manoeuvring from dock to dock; 2) the fairway navigation, which encompasses the entire voyage performance from origin to destination port including the high-sea, can be tightly coordinated; and 3) the operational efficiencies can be significantly enhanced by the technological advancement of the autonomous ships themselves. To propel the autonomous shipping forward, it is critical to perform valid demonstrations and simulations to quantify these potentials and benefits. The present study is initiated to explore the environmental benefit of the reduction in atmospheric pollutant emissions with the incorporation of autonomous shipping in the existing major international trading routes for dry bulk and tankers.

Autonomous ships have been on the agenda of marine community for some time. The concept was first mentioned in the 1980's by Schonknecht (1983), followed by the Japanese Intelligent Ship Project to develop automatic operation systems in the maritime field. Later, the Korea Research Institute of Ship and Ocean Engineering (KRISO) suggested the autonomous ships for maritime survey and surveillance to deal with national issues (KRISO, 2011). The recent wave of digitalization has further boosted the interest in leveraging the advantages of technology to address the current and future challenges in the global shipping industry. Many projects around autonomous ships had already been

initiated in the last decade (DNV GL, 2015; NFAS, 2017; SINTEF Ocean, 2020), with the primary objective to increase sea capacity so that more cargoes can be moved from road networks to waterways to alleviate the overcapacity of existing roads. In terms of implementation, Europe has been at the forefront of efforts to develop the necessary rules of autonomous ships, with Rolls-Royce and Kongsberg Maritime being the leading players. MUNIN (2016), Rolls-Royce (2016b) and MOL (2017) developed commercially and technically viable plans for ship navigation, machinery and all onboard operating systems at the concept level. Numerous research studies had also been performed to examine the various aspects with the practical applications of autonomous shipping, such as technological progress and path planning (Candeloro et al., 2017; Song et al., 2017; Singh et al., 2018; Topaj et al., 2019; Xia et al., 2019; Du et al., 2020; Garrido et al., 2020), manoeuvring control (Skjetne et al., 2004; Fossen, 2011; Zhao et al., 2014; Park, 2015; Dai et al., 2016; Zheng et al., 2017; Abdelaal et al., 2018), as well as collision avoidance and detection aspects (Statheros et al., 2008; Tam et al., 2009; Xue et al., 2011; Van Den Berg et al., 2011; Liu et al., 2016; Shen et al., 2019; Zhang et al., 2019; Huang et al., 2020).

Despite the extensive research work above, there remain some major research gaps on autonomous shipping based on our review. Firstly, prior work has focused more on the safe operation of autonomous ships with new digital technologies, such as sensors and artificial intelligence. However, the manner how these technologies can be operated in an integrated port-to-port manner to realise environmental gains has not been adequately addressed. Only a few pilot exercises have been conducted to assess the environmental performance of autonomous ships under controlled environment and short sea voyages, *e.g.,* DNV GL (2015) for a new efficient battery-propulsion system along the coast of southern Norway, and Kongsberg Maritime (2017) for an electric and zero-emission container ship that is scheduled to be put into service by 2022. Secondly, to our best

76 knowledge, no attempt has been made to investigate the impact due to potential adoption
77 of autonomous ships in major international trade routes so far. This limitation is
78 paramount, since 90% of the current world trade are carried by ships and it is predicted
79 that the tonne-mileage will rise to 74,000 billion in 2030 (Lloyd's Register et al., 2013).
80 Finally, the current researches are all based on a single ship, while a thorough assessment
81 will require the inclusion of an autonomous tonnage group.

82 To address the research gaps, we perform detailed simulations of the adoption of
83 autonomous ships in the major dry bulk and tanker shipping routes in this study, and
84 forecast the ship emissions in Years 2030 and 2050 using the Bayesian probabilistic
85 forecasting framework (Liu and Duru (2020) and Liu et al., (2021a)). With the framework,
86 important features of ship emissions with temporal and spatial variables can be
87 incorporated for coherent and unbiased forecasts. We noted that we had earlier employed
88 this framework to examine the adoption of autonomous ships during port stays (Liu et al.,
89 2021b). In this study, the framework is extended to the entire voyage and fleet from port-
90 to-port to account for the total emission abatement with the autonomous ship adoption
91 along the major dry bulk and tanker routes globally. Forecasting of port-to-port is of great
92 importance because high-sea sailing represents a considerable proportion of the overall
93 emissions, therefore its incorporating is critical for the planning of many stakeholders in
94 the industry. In this study, we adopt the Bayesian algorithm and establish the relevant
95 operational profile of autonomous ships, with considerations of ship types, cleaner future
96 viable fuels, engine efficiency improvement, and traffic volume. In addition, since the
97 adoption of autonomous ships shall be gradual, there shall be a co-existing period of
98 manned and autonomous vessels traversing the maritime routes simultaneously. Hence,
99 several phase-in scenarios are also included, and the mixed emissions are compared with
100 manned shipping only over the forecasting time horizon. Overall, we hope that the present

results on the environmental benefits can further aid the in-depth evaluation of the adoption and scaling up of autonomous ships in the shipping industry in the future.

2. Methodology

2.1 Site selection and Research Design

Simulations studies have been carried out for major shipping routes from origin to destination ports in the following: (a) three dry bulk carrier routes, i.e. Tubarao - Rotterdam, Tubarao- Kashima, and Hedland- Tianjin, and (b) three tanker routes, i.e. Ras Tanura- Qingdao, Ras Tanura- Galveston, and Houston- Singapore. The rationales for selecting these routes are multifold. First, they are core routes linking major continents and connecting important commercial shipping hubs. They also represent shipping flows with forecasted surges in traffic, which calls for more efficient and environmental-friendly handling. Second, the selected sea routes consist of varying voyage distance, transit time, and sailing conditions, thus representing nearly all the shipping scenarios of such trades. Finally, these origin and destination ports are major bulk cargo importers and exporters which together constitute a large percentage of global seaborn trade annually. Hence, these ports can reveal the magnitude of potential environmental benefits due to the adoption of autonomous ships.

There are two types of data collected in this study. The first type is the ship movement data (AIS data), which analyzes the sailing pattern of manned ships and designs the operation of autonomous ships. Ship movement data includes the geographical position, transmit time and sailing speed, which are sampled from AXSMarine[1] for the full year of 2020. To ensure that the algorithm captures the data in details, all the effective dynamic AIS observations on the voyages are retained after removing erroneous and duplicated records. In total, 36,000 final AIS observations with valid information are included this study for the data-processing,

[1] AXSMarine [website], https://public.axsmarine.com, (accessed 6 January 2021).

125 calculation and analysis, of which high-sea and port movements accounted for 85% and 15%,
126 respectively. Based on these findings, approximately 15% of marine fuel consumption for the
127 fleet occurred in ports and anchorages where ships often operate in very inefficiently in their
128 port call processes, *e.g.*, frequent speed changes with abrupt stoppages, prolonged slow-speed
129 sessions to wait for berth allocation, and avoidance of collision with nearby ships or floating
130 objects. Even during high-sea voyages, unproductive maneuvers could often be identified from
131 the observations, such as unnecessary speed variations and frequent accelerating and
132 decelerating operations. The observed sailing pattern of manned ship creates energy surges
133 typically, which leads to sub-optimal combustion processes and an increase in specific fuel
134 consumption per unit of power produced (Faber et al., 2012).

135 Comparatively, autonomous shipping is modelled using an optimized operational
136 profile enabled by the advanced technology on board, with a constant sailing speed on the high-
137 sea and a gradually decreased speed pattern in ports when approaching the harbor. Figure 1
138 provides a demonstration for the profile, which a proposed speed is designed based on real AIS
139 data along the selected sea routes from January to December 2020. Currently, ships with
140 different types and sizes sail with different operational speeds. A typical large tanker is
141 designed to sail at ~15 knots, whereas a large dry bulk carrier at ~13-14 knots. In addition,
142 large ships are usually associated with a higher speed than smaller ships due to their design
143 constraints and hence the actual sailing speed may vary considerably among the different sizes.
144 For example, a typical 200,000 Dead Weight Tonnage (DWT) crude oil tanker has an average
145 sailing speed of 15 knots, whereas a 60-79,999 DWT crude oil tanker has a sailing speed of 13
146 knots. Such variations are important in determining the navigational characteristics of
147 autonomous ships because a single speed for all ships would affect the ship type differently.
148 Hence, differentiated proposed speed is essential to be assigned to ships of types and sizes.

149 After establishing the proposed speed, the modelling proceeds to modify the existing

ship movements by incorporating the sailing profile of autonomous ships. First, a complete voyage is divided into numerous partial ship trajectories with the time and speed information recorded. Then, the partial trajectories are calibrated by substituting new speed information with corresponding changes made in the time duration for that trajectory. It is important to adjust the time interval to prevent overestimation or underestimation of the distance covered due to the modified version of sailing speed. This can be done by using the Haversine Rule, which calculates the distance between two points on Earth. For example, given a sailing distance of x nautical miles from origin to destination port, the x nautical miles are split into k equally partitioned ship trajectories. The coordinates are recorded to determine the distance travelled for each trajectory. As a result, there are k modifications for each step, then the problem is to find an efficient way to convert the speed to ensure the assigned values are reasonable estimates.

In this study, the voyage time including both the sailing time on high-sea and within ports serves as the benchmark to evaluate the proposed scenario. This is because the voyage time reflects the shipping demand on the selected types of trade. Changing the relative performance of autonomous ships below the benchmark, *e.g.,* shorter voyage time, would simply render the current fleet less efficient. Based on our assumptions, the simulations with autonomous shipping result in a shorter turnaround time for all the study areas and ship types, which is consistent for the purpose of our analysis. The final output is a sequence of partial ship trajectories with newly embedded speed and time values. Moreover, since the existing sea routes demonstrate reliable and realistic trading choices with en-route bunkering stops, the scenario of autonomous ships shall also follow the same ship trajectories.

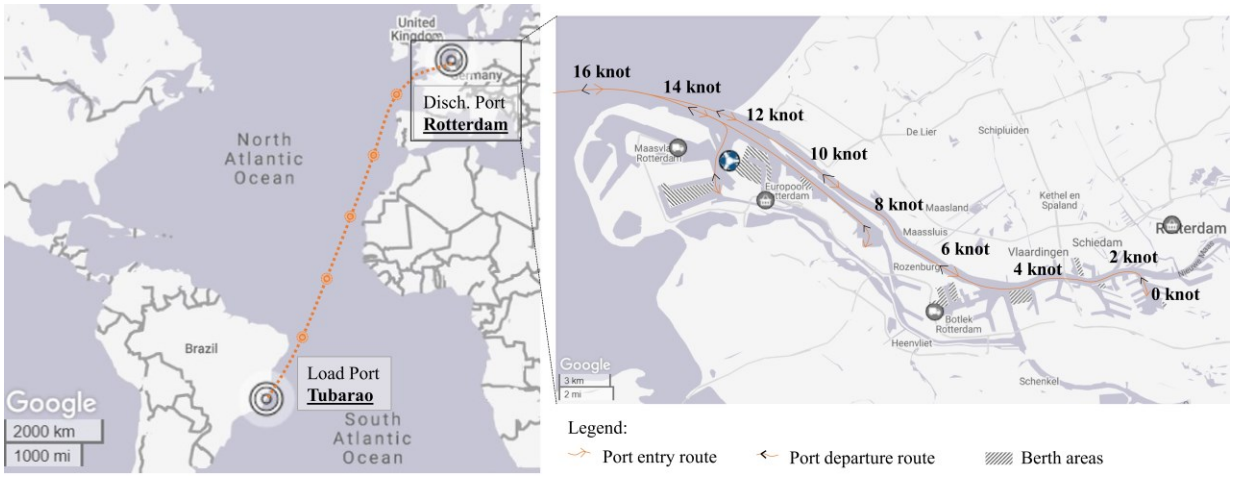

Fig.1. Concept of autonomous ship navigation (Tubarao to Rotterdam).

The second data type is the historical ship traffic data, which tracks the development over time on the selected routes and forecasts the future traffic volume in Years 2030 and 2050. The data are collected from AXSMarine for the period of 2013 to 2020 monthly. Specifically, time series forecasting is applied to establish a function based on the historical data which can then be used to predict future values. Instead of basing on a single forecasting technique, this study adopts an ensemble approach which combines the results of several forecasting models, namely the AutoRegressive Integrated Moving Average (ARIMA), Exponential Smoothing (ETS), Holt-Winters (HW), and Neural Network Auto-Regressive (NNAR).

The computation procedures are given as follows. First, the available historical traffic data are split into training, validation and test subsets based on a 40-20-40 ratio. The training subset allows the models to learn the real properties of the input, build up the prediction models, and subsequently predict on the validation subset. Then, multiple accuracy metrices are established to give an unbiased assessment of the trained models, tune the parameters, and select the finals models with lower forecast errors on the validation dataset. Subsequently, the test subset is again split 70-30 into two parts (test1, test 2). The test1 trains the ensembles on a completely unseen real-world data and adjusts the weights (normalized to 1) accordingly. The

test2 evaluates different ensemble schemes on their performance between actual and forecasted results and filters the best fitted ensemble model. Finally, the selected ensemble is used to predict the future traffic on the sea routes.

Overall, this process can be expressed using the following mathematical formulas. Suppose the actual data are $\mathrm{Y} = \{y_1, y_2, \dots, y_N\}$ and the forecast results are $\hat{\mathrm{Y}}^{(\mathrm{i})} = \{\hat{y}_1{}^{(i)}, \hat{y}_2{}^{(i)}, \dots, \hat{y}_N{}^{(i)}\}$ based on the i^{th} time series forecasting method ($i = 1,2,..,N$). Then, the ensemble series obtained from combining these n forecasted series are:

$$\hat{\mathrm{Y}}^{(\mathrm{c})} = \{\hat{y}_1{}^{(c)}, \hat{y}_2{}^{(c)}, \dots, \hat{y}_N{}^{(c)}\} \quad (1)$$

$$\hat{y}_k{}^{(c)} = w_1\hat{y}_k{}^{(1)} + w_2\hat{y}_k{}^{(2)} + \cdots + w_n\hat{y}_k{}^{(n)} = \sum_{i=1}^{n} w_i\hat{y}_k{}^{(i)};\ \forall k = 1,2,\dots,N \quad (2)$$

where w_i is the weight assigned to the i^{th} time series forecasting model.

The calculated results are given in details in the Appendix. Particularly, the performance of the ensemble model is superior to the best single model for different sea routes in most of the accuracy metrics. This can be attributed to the fact that the shipping industry is volatile in nature, hence it is very difficult for a single model to capture all the underlying trends of the data. Since the ensemble method offers a diverse pool of models, each can learn a different set of temporal knowledge and together their ensemble predictions can aggregate the forecasting strengths of the contributing models and enhance the overall forecasting accuracy. In addition, we base the future ship size distributions of dry bulk carriers and tankers on the information given in the IMO report (2020). This is to ensure the potential changes in ship sizes are well reflected in the emission forecasts and the simulations represent the realistic sailing environment as much as possible.

2.2 *The Bayesian probabilistic forecasting algorithm*

The Bayesian probabilistic forecasting algorithm provides a platform for different data

sources to merge and form probability distribution. In other words, the sampled movements of conventional ships can be transformed into time distributions and updated by newly calibrated movements of autonomous ships to form the posterior distribution as:

$$P(\Theta|y_t) = \frac{P(y_t|\Theta)P(\Theta)}{P(y_t)} \propto P(y_t|\Theta)P(\Theta) \quad (3)$$

where $P(\Theta|y_t)$ is the posterior time distribution given the sampled ship movement data y_t, t is the time of the data, $P(y_t|\Theta)$ is the likelihood function, and $P(\Theta)$ is the prior time distribution. The denominator is a normalizing constant which ensures that $P(\Theta|y_t)$ integrates to unity.

The prior distribution is based on the posterior distribution of an independent pilot study conducted from June to December 2019 along the selected sea routes. Due to the absence of real prior information, the prior distribution of the pilot study assumes an unform distribution, i.e. $f(\Theta)$ = constant. The lower and upper bounds $[a_{min}, b_{max}]$ denote the historical minimum and maximum time to travel on the routes according to published records (AXSMarine, 2021), and assume equal probability for a ship to consume any amount of time within the range depending on ship condition and real sailing environment. The ship movement data y_t sampled during the pilot study is fed into the computation as new observations to update the prior distribution. In this case, the data points are fitted with multiple candidate distributions using the Anderson-Darling test at 0.05 significant level. Overall, the log-normal distribution is observed with the highest p-value and further validated by the probability plot, which demonstrates good alignment of datapoints in a straight line. The transformed log-scale is:

$$P(y_0|\Theta) = \frac{1}{\sqrt{2\pi}\sigma_{y_0}} exp\left[-\frac{\left(y_0 - y_0(\theta)\right)^2}{2\sigma_{y_0}^2}\right] \quad (4)$$

Hence,

$$P(\Theta|y_0) \propto \frac{1}{\sigma_{y_0}} exp\left[-\frac{\left(y_0 - y_0(\theta)\right)^2}{2\sigma_{y_0}^2}\right] 1\{\ominus \in [a_{min}, b_{max}]\} \quad (5)$$

where (θ, σ_{y_t}) are the mean and standard deviation of y_t.

After the pilot study, the posterior distribution derived from Eq. (5) is applied as the prior distribution in the current research. A completely new set of ship movement data y_1 are collected from January to December 2020 to form the likelihood function and update the prior knowledge. In this case, y_1 embeds the features of autonomous ship navigation scenario with corresponding modifications made in speed and time. The calibrated ship movements can be converted into time distributions. The Bayesian modeling adopts an ensemble of functions, each representing an independent time distribution for a specific speed interval *e.g.,* 1-2 knots, 2-3 knots, …, and 14-15 knots. The likelihood function of the final time distribution is a probabilistic combination of those from individual time distributions grouped by their respective speed intervals. This result is then combined with the prior distribution (Eq. (5)) to formulate the updated posterior distribution of autonomous ships as:

$$P(\Theta|y_t) = \frac{1}{\sigma_{y_0}\sigma_{y_1}} exp\left[\frac{-\left(y_0 - y_0(\theta)\right)^2}{2\sigma_{y_0}^2} - \frac{\left(y_1 - y_1(\theta)\right)^2}{2\sigma_{y_1}^2}\right] \quad (6)$$

In the calculation of the posterior distribution, the Markov Chain Monte Carlo (MCMC) Metropolis-Hastings algorithm is employed to produce a sufficiently large number of samples from the posterior distribution function described by Eq. (6). The following illustrates the MCMC algorithm performed for $\mathrm{t} = 1, \ldots, \mathrm{t} - 1$:

1. Initialize the starting state Θ_t at $\mathrm{t} = 0$
2. Draw a sample Θ_* from a normal proposal distribution $\Theta_* \sim q(\Theta_*|\Theta_t)$. Note that this proposal is now a function of the previously drawn sample Θ_t, at time step t.
3. Decide whether the computation should accept this new state by calculating the acceptance ratio $r(\cdot)$ and probability $\alpha(\cdot)$, as shown by Eqs. (7) and (8) below.

$$r(\Theta_*\Theta_{t-1}) = \frac{Posterior(\Theta_*)}{Posterior(\Theta_{t-1})} = \frac{p(\Theta_*|y_t)\, q(\Theta_{t-1}|\Theta_*)}{p(\Theta_{t-1}|y_t)\, q(\Theta_*|\Theta_{t-1})} \quad (7)$$

$$\alpha\left(\Theta_{*,}\Theta_{t-1}\right) = min\{r(\Theta_*, \Theta_{t-1}), 1\} \quad (8)$$

4. Draw a random number from the uniform distribution $u \sim U(0,1)$.
5. Let $\Theta_{t+1} = \Theta_*$ if $u < \min(1, \alpha)$, and $\Theta_t = \Theta_{t+1}$ otherwise.
6. Repeat steps 2 and 3 until the samples converge. In this calculation, approximately 8,000 postburn-in samples are used for inference and forecast.

The Bayesian-based model relates the posterior time distribution with the ship parameters specified in Eq. (9) to calculate the ship emission for a single voyage, which is then combined with the forecasted traffic to obtain the total emissions in any forecasting year. The entire calculation process is summarized in a study flowchart shown in Figure 2.

$$E_{i,j,k,l,m} = \sum_{i=1}^{n} VAN_m \times P_j \times LF_{j,l} \times T_{j,l} \times EF_{i,j,k} \times CF_{i,k} \times LLAF_j / 10^6 \quad (9)$$

where *i,j,k,l,m* and *n* represents the pollutant species, engine type, fuel type, operating mode, ship type and number of AIS observations, respectively. *E* is the estimated emissions (t); *VAN* is the total ship traffic on each selected route; *P* is the engine power (kW); *LF* is the load factor; *CF* is the control factor for any emission reduction measures (Table A.3); *T* is the posterior time distribution (h); *EF* is the emission factor (g/kW·h, Table A.4-A.10); and *LLAF* is the low load adjustment factor.

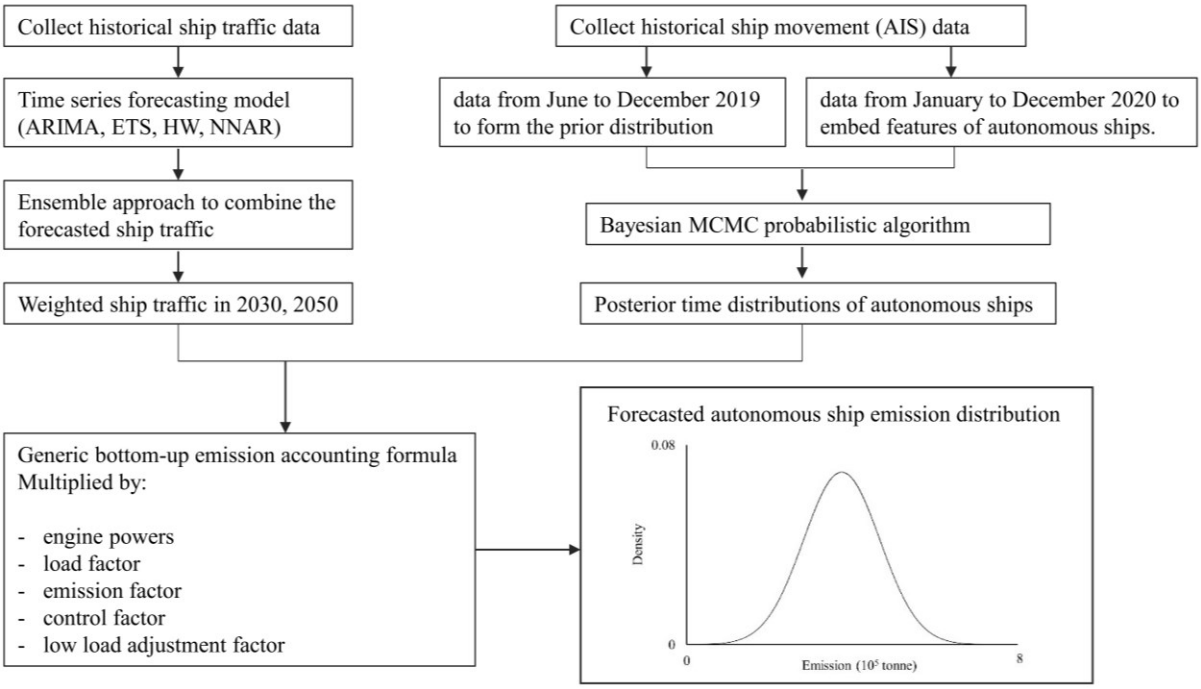

Fig.2. Study flowchart.

3 Results and Discussion

3.1 Emission results

The simulated results of autonomous ships, shown in Figure 3, show that the voyage time savings on the selected sea routes increase in the smaller tonnage groups before rising rapidly and then falling gradually for the larger tonnage groups. The savings are generally higher for tankers than dry bulk carriers, and the difference is largest for the 60,000-79,999 tonnage group but reduces substantially for larger tonnage groups. This ship type difference is similar for autonomous ships, which superior navigational performance can be realized together with the emission reduction in atmospheric pollutants.

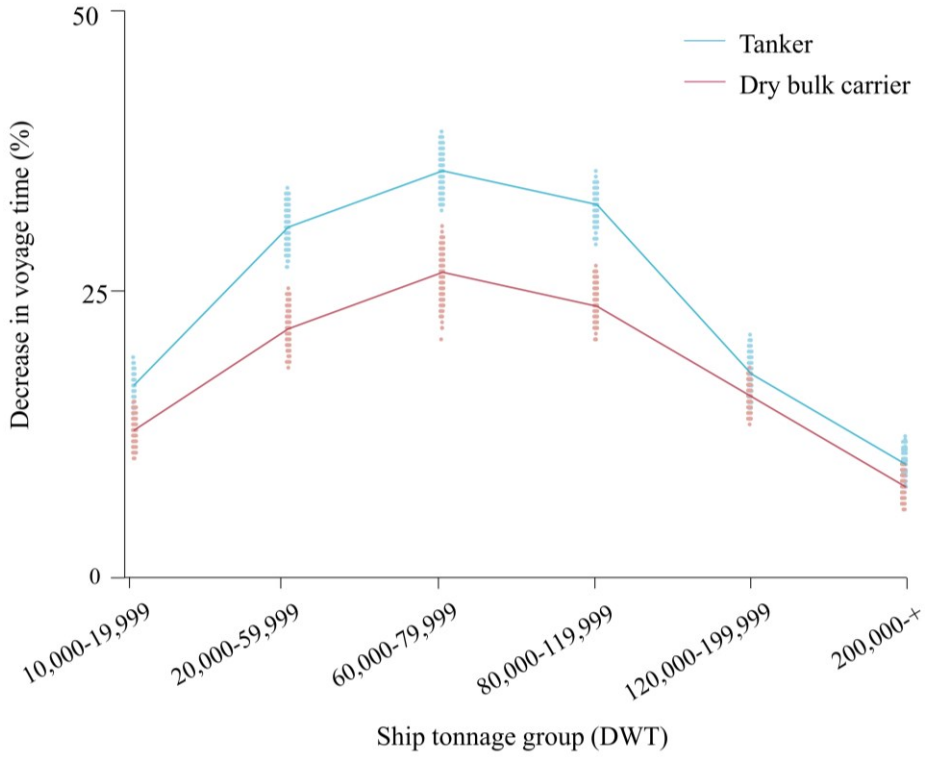

Fig.3. Decrease in voyage time by ship size group (the solid line shows average decrease and each point shows change in each ship).

Ship emissions in Year 2020 ranged from 4.45 x 10^4 to 9.99 x 10^4 ton for tankers, and from 2.63 x 10^4 to 3.92 x 10^5 ton for dry bulk carriers. The above number in ton is the sum of some major pollutants, which includes CO_2, SO_X, NO_X, PM, CO, and CH_4. We note that the emission results in 2020 only include the conventional ships, while the projections in 2030 and 2050 reflect the 50% autonomous ship phase-in scenario. The future scenarios are based on the forecasted ship traffic as detailed in Section 2.1. Figure 4 shows that between 2020 and 2030, there is 90% probability that ship emissions will decrease by 20-49% for tankers and 11-30% for dry bulk carriers, reaching a level of 3.37 x 10^4 ton (Tubarao to Rotterdam), 1.92 x 10^4 ton (Tubarao to Kashima), 3.50 x 10^5 ton (Hedland to Tianjin) for tankers, and 2.22 x 10^4 ton (Ras Tanura to Qingdao), 3.66 x 10^4 ton (Ras Tanura to Galveston), and 8.03 x 10^4 ton (Houston to Singapore) for dry bulk carriers. Ship emission gains varied substantially across sea routes

because large cross-route variations exist in how much ship-specific performance improved. The variation can be attributed to the sailing route choice i.e. bunkering stop priorities and distances, and the voyage time savings for the individual ship size group. For example, about two-thirds of the forecast reductions in dry bulk carriers and more than three-quarters of those in tankers are due to the voyage time reductions and optimized speed configuration of autonomous ships. The voyage time reductions of autonomous ships are uneven across the different ship sizes, with percentage averaging ~22% in small tonnage groups (20,000-59,999 DWT), larger in middle-size ships (60,000-119,999 DWT), but smaller in bigger vessels (120,000-199,000 DWT), especially in the tanker segment. The notable exception is the dry bulk carrier route from Hedland to Tianjin, where the emission in 2050 is projected to stagnate or increase relative to 2020, with at least 35% probability if the current traffic continues to grow with no additional action. Going forwards, environmental benefits could be realized in most of the sea routes, reaching or surpassing 4.52 x 10^4 ton (~39% less compared to 2020) for tankers and 1.49 x 10^5 ton (~23% less compared to 2020) for dry bulk carriers by Year 2050 with over 50% probability. In a few sea routes (Tubarao-Kashima; Ras Tanura-Qingdao), the emissions of autonomous ships reach 1.64 x 10^4 ton for dry bulk carriers and 1.59 x 10^4 ton for tankers at 90% probability, yet they represent drastic reductions of 37-64% relative to 2020.

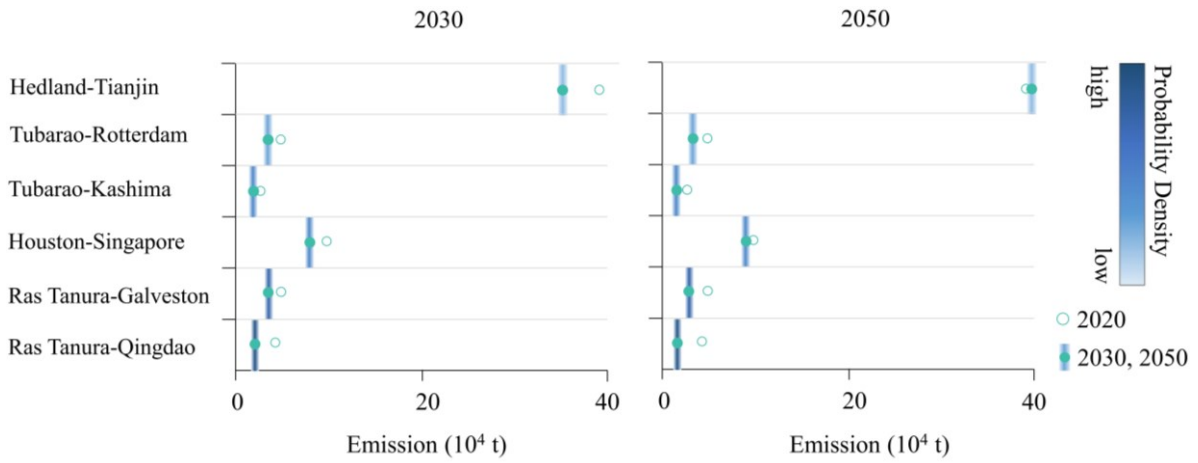

Fig.4. Posterior distribution of projected ship emissions (Year 2030, 2050).

A larger relative reduction in ship emissions can be expected in tankers than dry bulk carriers, because their voyage time is forecasted to shrink more comparatively with noticeable improvement in the sailing performance of small and middle-size tankers. The difference is more pronounced for tonnage ranges between 20,000-119,999 DWT, whereas, in very-small and very-large ships, the relative effects are similar in dry bulk carriers and tankers. For example, the autonomous tankers have an estimated 39% reduction in emissions between 20,000-119,999 DWT, compared to 28% in dry bulk carriers of the same size. In absolute terms, the total emission reduction due to the adoption of autonomous ships is overwhelmingly in the tonnage range between 60,000-119,999 DWT which contributes 61% of the total gains.

As a result of these trends, the emission difference across the different ship-size groups increases between 2020 and 2050. For example, between the middle-size ships i.e. 60,000-119,999 DWT and bigger vessels i.e. 120,000-199,999 DWT, the difference increased from 1.15×10^3 to 1.91×10^3 ton for tankers, and from 1.10×10^3 to 1.85×10^3 ton for dry bulk carriers. The widening occurs because the current sailing profile of small- and middle-size ships are more volatile with speed surges. Because the engine power bears a nonlinear relationship with the speed, therefore the sailing profile has a significant influence on the fuel consumption and the engine emissions. In other words, improving the time and speed features of small- and middle-size ships can yield a higher degree of emission reduction compared to the larger vessels, and is thus highly beneficial towards the planning of future regulations and ship deployment. Another difference is that the bigger vessels between 110,000-200,000 DWT, which currently takes up a significant portion of the world fleet (~17% for tankers and ~15% for dry bulk carriers in 2018) are expected to yield greater benefits with the adoption of autonomous ships by 2050. This is due to their growing shares in the fleet in the future (~53% and 39%, respectively (IMO, 2020)) and hence longer-term implications on the environment.

In the literature, some research studies (*e.g.,* Lindstad et al. 2012) had noted that bigger

vessels tend to yield better environmental performance per tonnage due to the economy of scale. The findings in this study, however, show that the autonomous progress would come at the cost of rising ship-size divergence, and the future emission outlooks will be associated more with fleet-level compositions than individual ship characteristics. Thus, steps should be taken in the future to focus on ship-size inequalities as part of worldwide ship emission accounting systems.

3.2 Emission result by phase-in rates and fuel types

As stated earlier, there is a high probability that future emissions by autonomous ships will continue to decrease from 2020 to 2050 for the selected sea routes. To investigate the opportunity space of such technology, this study constructs a series of scenarios, each defining a specific combination of potential reductions based on two types of influential drivers: the autonomous ship phase-in rate, i.e. 25, 75, and 100%, and alternative fuel type. In this section, we focus on three types of future viable fuels, namely the Liquified Natural Gas (LNG), Very Low Sulphur Fuel Oil (VLSFO), and methanol. For each scenario and sea route, we evaluate whether the specific combination of reductions can achieve larger emission reductions by comparing with 2020, which is the baseline year for measuring emission progress, as well as the overall emission results of autonomous ships in Section 3.1 (referred to as S0 hereafter).

Figure 5(a) plots the posterior probability of the emission reductions with 25% phase-in rate, which shows that a decline in ship emissions over the forecasting period 2050 is less than 50%, i.e. an increase is more likely due to projected ship traffic growth from Hedland to Tianjin; 75-90% for tankers from Houston to Singapore and dry bulk carriers from Tubarao to Kashima; 99% for dry bulk carriers from Tubarao to Rotterdam; and more than 99% for tankers from Ras Tanura to Galveston and Ras Tanura to Qingdao. Figure 5(b) maps the posterior distributions of percent reduction from 2020 to 2050. The relative reduction in ship emissions, compared to the 2020 level, ranges from an average of 17% for dry bulk carriers to more than

25% for tankers. The largest reduction in ship emissions for tankers is most likely to be from Ras Tanura to Qingdao (75%), followed by Ras Tanura to Galveston and Houston to Singapore; and for dry bulk carriers, the largest reduction is likely from Tubarao to Kashima (35%), followed by Tubarao to Rotterdam and Hedland to Tianjin.

The relatively minor reduction in some of the sea routes, such as the dry bulk carrier route from Hedland to Tianjin, and to some extent the tanker route from Houston to Singapore, is a consequence of having both a long duration of speed rises and large proportion of big vessels that are more than 200,000 DWT in the traffic. In some parts of the voyage, the observed sailing speed is more than twice of the other legs of the journey. In contrast, the routes from Ras Tanura to Qingdao and Ras Tanura to Galveston have smaller speed rises and shorter times, and, hence, an overall decrease of more than 12 times compared to Hedland to Tianjin and Houston to Singapore. At the same time, Tubarao to Rotterdam and Tubarao to Kashima had the longest duration of speed rises but with a smaller proportion of large vessels in the fleet. Hence, the overall relative emission reduction falls between the sea routes with moderate-to-high (for example, Ras Tanura to Qingdao and Ras Tanura to Galveston) and moderate emission savings (for example, Houston to Singapore and Hedland to Tianjin).

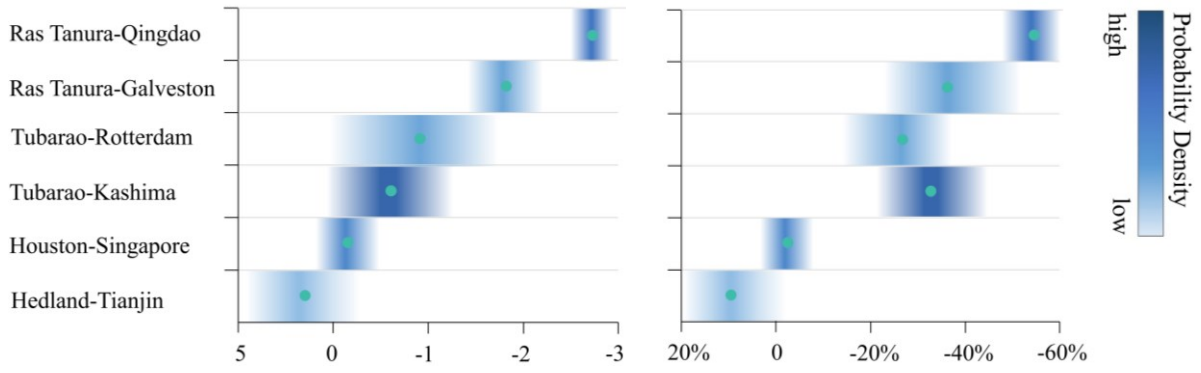

(a) Emission reduction (10^4 t). (b) Emission reduction (%).

Fig.5. Posterior distribution of emission reduction at 25% phase-in rate.

Taken across all the sea routes in this study, the amount of emission reduction due to autonomous ships is expected to grow with higher phase-in rates (Figure 6(a)). For example, with 75% autonomous ships in the fleet, there is 90% probability that the total ship emission will be reduced by at least 27% for tankers and 18% for dry bulk carriers by 2030. At the extreme, if fully autonomous ship navigation would be adopted in every sea route, the overall emission in 2030 would decline by 35-60% for tankers and 25-41% for dry bulk carriers with 50% probability. By 2050, the median decline would be 49% for tankers and 34% for dry bulk carriers compared to 2020. The relative effect of the phase-in rate on ship emissions can be compared with the S0 results presented in Section 3.1. Under the S0 scenario, there is a projected reduction in ship emissions between 2020 and 2050 in five of the six sea routes, with the reduction ranging from 11-62% for tankers and -2-36% for dry bulk carriers of the 2020 levels. A higher rate of autonomous ships adoption can therefore further accelerate the reduction in future emissions in all the sea routes on top of the projected S0 decline, and can even reverse the rising trend in the dry bulk carrier route from Hedland to Tianjin (Figure 6(b)). At the regional level, the accelerated adoption of 100% can help delay or prevent between 2.58 x 10^4 ton in the tanker routes and 7.30 x 10^4 t in the dry bulk carrier routes over the analysis period of 2050. In sea routes and ship types where the emission reduction relative to S0 has a posterior probability of at least 50%, the reduction is lowest for tankers from Ras Tanura to Qingdao and for dry bulk carriers from Tubarao to Kashima. The additional benefit is the largest from Hedland to Tianjin and from Houston to Singapore, with posterior median estimates for tankers and dry bulk carriers ranging from 7.22 x 10^4 to 3.34 x 10^5 ton, a level that is above and beyond the reduction under the S0 scenario. The posterior median decrease is also more than 5.26 x 10^4 ton for both ship types in Tubarao to Rotterdam and Ras Tanura to Galveston, equivalent to a minimum reduction of 16% compared to S0.

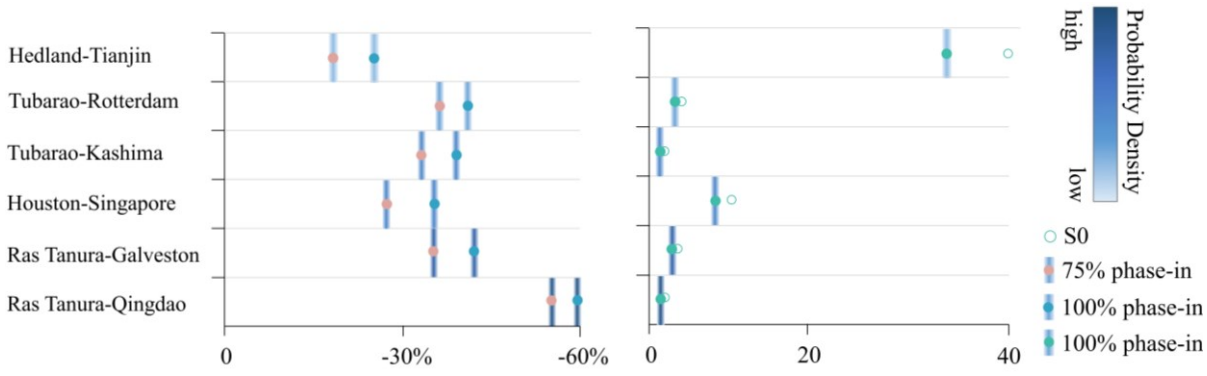

(a) Emission reduction in 2030 (%). (b) Emission in 2050 (10^4 t).

Fig.6. Posterior distribution of ship emissions (Year 2030, 2050).

Another important driver of ship emission is the fuel choice. From Year 2020 onwards, it has been made mandatory to switch from the high-Sulphur 3.50% bunker fuel to cleaner fuels with maximum 0.50% m/m Sulphur content. We have included the effect of regulation by simulating the complying fuel-mix in the ship emission calculations. Previous studies on ship emission pointed out that the transition to low-Sulphur fuels can bring a reduction of ship emissions and a reduced impact on human health (Tao et al., 2013; Contini et al., 2015). However, the recent study by Contini and Merico (2021) highlighted that there are still relevant impacts that require further mitigation efforts. In this study, we simulate the impact of cleaner fuels in combination with the adoption autonomous ships. Figure 7 presents the comparison of percent reduction in emissions between different fuel scenarios in the forecasting years - LNG only, VLSFO only, and methanol only. In relative terms, the LNG advantage is the largest in the tanker routes between 2020 and 2030 at 75% phase-in rate (49% reduction (40-62%) with LNG, followed by 38% (25-54%) with methanol and 30% (17-48%) with VLSFO) as well as dry bulk carrier routes (41% (31-48%) with LNG, 28% (17-35%) with methanol and 18% (6-26%) with VLSFO). A full adoption of automation in the fleet combined with LNG as combustion fuel has an even larger impact in 2050 than that of 2020 (~59% reduction in the

441 tanker routes and ~45% in the dry bulk carrier routes) and S0 (~26 and 20%, respectively), and
442 is therefore the most efficacious approach. In particular, the tanker route from Ras Tanura-
443 Qingdao is forecasted to have an emission greater than 1.08 x 10^4 ton in 2050 with probabilities
444 of over 50%, which is approximately 75% less than the amount in 2020. There is also a
445 noticeable decrease of emission in the dry bulk carrier route from Tubarao to Kashima during
446 the 2020-2050 period (from 2.63 x 10^4 to 1.17 x 10^4 ton), with a probability of 50%. As a result,
447 its emission level by 2050 is projected to fall by 56% in the fuel scenario of LNG, followed by
448 Tubarao-Rotterdam (53%) and Hedland-Tianjin (28%).
449 Of the remaining two fuel choices, the scenarios with methanol generally have a higher
450 reduction ratio than VLSFO. Similar to LNG, the projected emissions from VLSFO and
451 methanol are declining rapidly in most of the sea routes, from very high reduction in tankers,
452 with some dry bulk carriers on track to achieve a reduction of one-third by 2030. These trends
453 are expected to continue into 2050, when all routes have a 2-17% reduction at 100% phase-in
454 rate compared to 2020, and at least 5-10% emission reductions compared to the levels of S0.
455 The results imply that all tankers and dry bulk carriers can achieve lesser emissions compared
456 to the baseline 2020, and a decline of more than the levels of S0 scenario, though ambitious, is
457 within reach by utilizing cleaner fuels. They also point to the situation that the emission control
458 strategy has to be implemented on a fast-track in successful scenarios for each sea route, which
459 measures the degree of necessity of phasing-in autonomous ships at the fast rate to achieve the
460 emission goals.
461

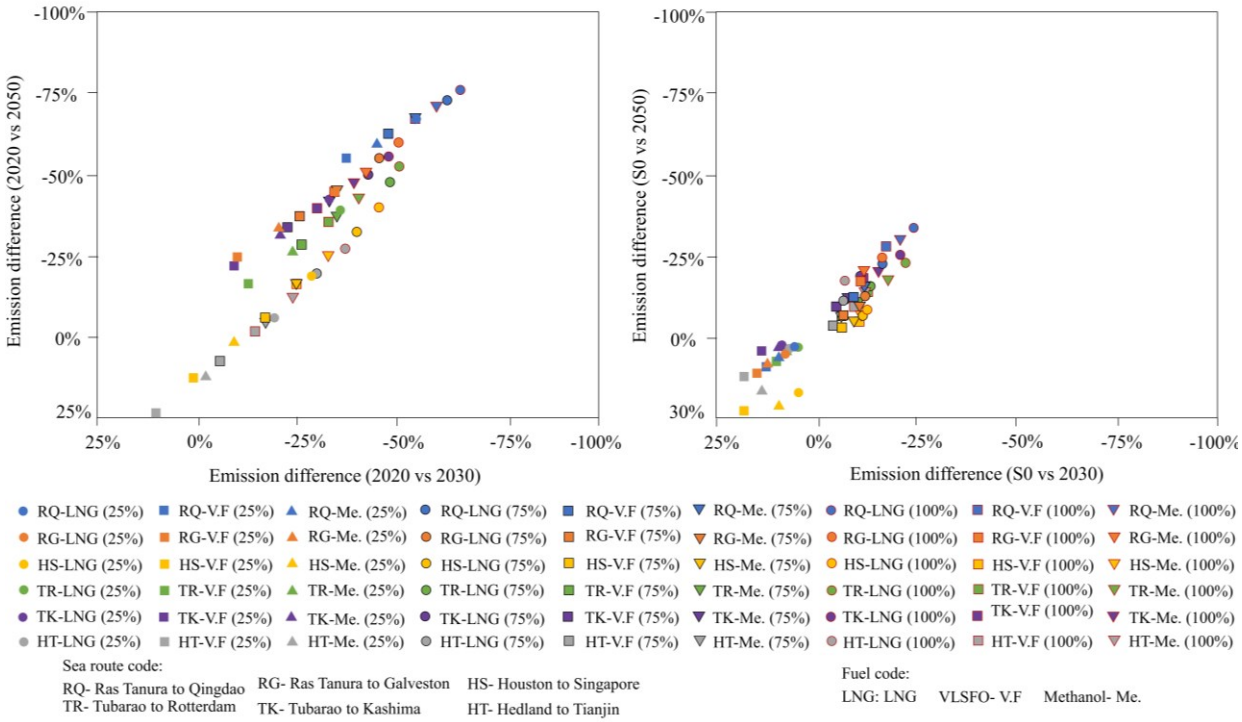

Fig.7. Comparison of percent change in emissions between different fuel scenarios. Numbers in bracket *e.g.*, 25, 75, and 100% represent the autonomous ship phase-in rates. Points represent the posterior median emission with respective phase-in rates).

We also investigate the ship emissions by pollutants and their rate of change over the period of 2020-2050 for various fuel types, shown in Figure 8. There are substantial variations in the decline rate, with the posterior median rate ranging from 38 to 80% in tankers and 22 to 78% in dry bulk carriers. SO_X is the fastest declining pollutant (-80% in tankers and -78% in dry bulk carriers), followed by PM (-72, -67%), NO_X (-65, -58%), CO_2 (-45, -33%), and CO (-35, -20%), with over 50% probabilities. Among all, the CH_4 emission in 2050 and its growth rate are lower than those by other studies (Liu & Duru, 2020; Liu et al., 2021a, b), with a moderate-to-medium decrease of 30 and 40% in tanker and dry bulk carrier routes by 2050, respectively. This difference might be attributed to the adoption and simulation of a diesel-cycle and high-pressure engine in autonomous shipping, which eliminates most of the methane slip (MAN Diesel & Turbo, 2016). On a CO_2-equaivalent (CO_2e) basis using the 100-year

478 Global Warming Potential (GWP) factor of 1 for CO_2 and 25 for CH_4, the overall CO_2e
479 emissions in 2050 are forecasted to decline by 9-64% for tankers and 4-36% for dry bulk
480 carriers in different sea routes compared to 2020. The median decline would be 39% for tankers
481 and 23% for dry bulk carriers. On top of that, there are notable differences in the reduction rate
482 of pollutant types attributable to LNG versus VLSFO and methanol. For example, LNG can
483 yield more than 1.5 times the decline of CO_2 (40%) and NO_X (74%) as compared with VLSFO
484 (20% for CO_2 and 29% for NO_X). Similarly, the projected decrease of SO_X, PM, CO and CO_2e
485 in tankers and dry bulk carriers with LNG is also substantially higher than methanol.
486 The sea routes in this study have different options to achieve emission reductions by
487 2050. However, each route needs to examine its emission control strategy carefully, with the
488 possible outcome in the present study ranging from 10% excess emissions to 71% reduced
489 emissions. A clear choice is the switch to cleaner fuels. To provide a general picture, an
490 emission abatement of 28-30% can be realized with the use of LNG for conventional ships by
491 2050 compared with the 2020 level across various trading routes; 13-15% with methanol; and
492 7% with LSFO. Significant higher emission cuts can also be achieved when combining the
493 alternative fuel mixes with autonomous ships, reaching a higher range of 45-59% emission
494 reductions by 2050. In addition, the projections highlight the importance of efficient port-call
495 processes to reduce emissions. The results imply that a significant amount of ship emission
496 occurs during manoeuvres in ports. With the efficient navigation of autonomous ships, the total
497 emissions are expected to be curbed by 32-48% across ports by 2050 compared with 2020.
498 This finding is critical because maritime emissions have a severe impact on local air quality of
499 port-cities nearby the harbours (Merico et al., 2019). Given the vast amount of time that ships
500 spend at docks, the fuel quality also has a large impact on the total emissions in ports. Hence,
501 further studies on the rigorous comparative analysis of emission outcomes and their energy and
502 technology system determinants, similar to the analysis carried out in this study, will be

503 essential to monitor the evolutionary trends and advocate the needed policies and actions.

504

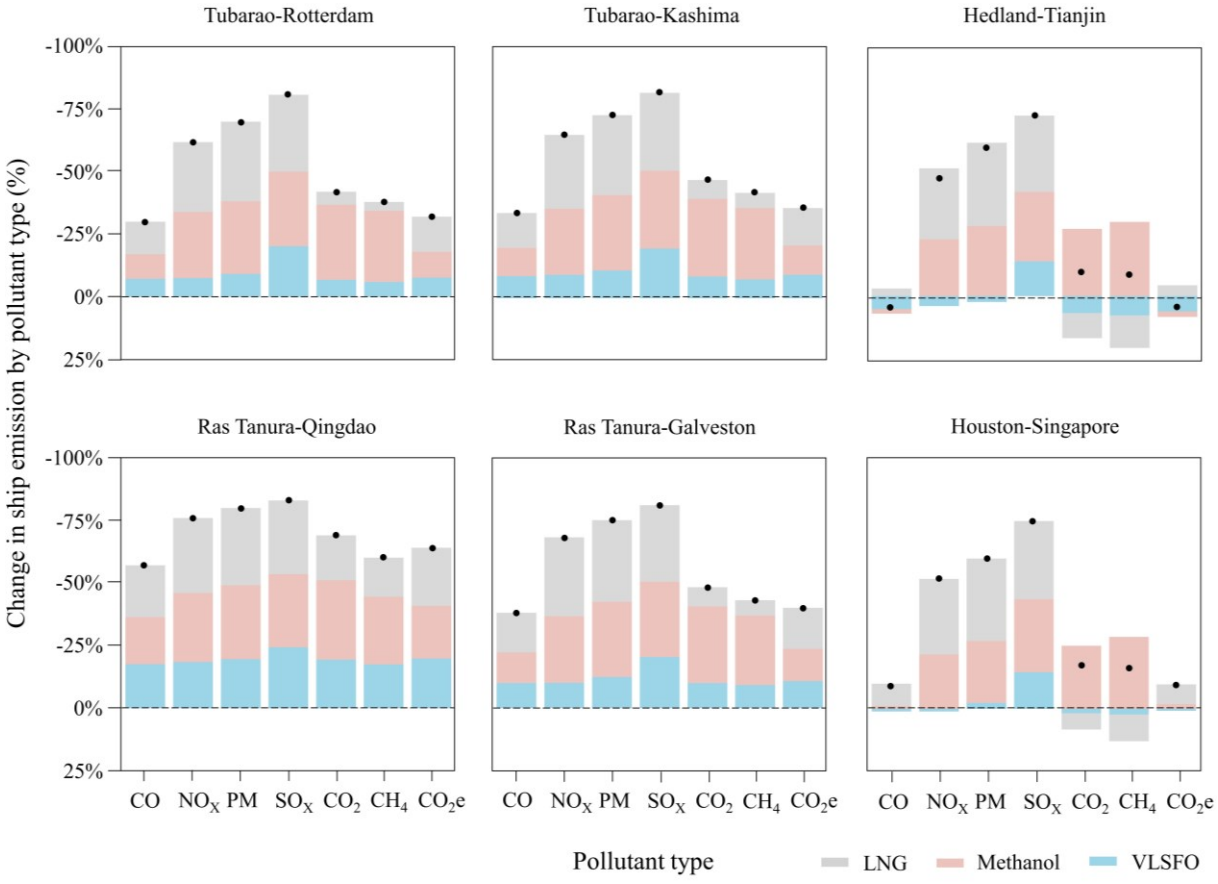

505

506 **Fig.8.** Change in emissions between 2020 and 2050 by pollutant type. The black dots
507 represent posterior median change in emissions for each set of bars. The different color
508 represents the ratio of decrease/increase in emissions by different fuel types.

509

510 **4 Conclusion**

511 This study develops the Bayesian probabilistic forecasting algorithm to simulate the
512 total abatement of pollutant emissions due to the progressive adoption of autonomous ships
513 from now to Year 2050 along three major international tanker and dry bulk carrier sea routes.
514 The methodology has the advantages of quantifying the uncertainty involved, beyond the
515 subjectivity and expert-judgement in conventional ship emission accounting studies. The use
516 of the modelling framework enables the quantification of the emission outcomes across various

517 sea routes, ship size, and speed patterns, which, because of the lack of real navigational data,
518 may not be possible otherwise. The simulation results show that the progressive adoption of
519 autonomous ships has a high potential to cut the emissions significantly by 11-64% for tankers
520 and -2-37% for dry bulk carriers in Year 2050 compared to 2020. The findings, together with
521 other ship-specific factors such as maritime regulation, port control and infrastructure that are
522 needed for delivering the positive outcomes, can aid the related planning and advocacy of
523 autonomous shipping for tankers and dry bulk carriers in the future. In addition, the results also
524 point to the important role of faster phase-in rate for autonomous ship adoption, i.e. 75 and 100
525 instead of 25%, as well as cleaner fuels, i.e. LNG, VLSFO, methanol, and up to about half of
526 the ship emissions attributable to CO_2 and 65% of emissions attributable to NO_X could be
527 reduced progressively from 2020 to 2050. Both SO_X and PM emissions will also have the
528 highest reduction, with the posterior median declining by at least 72-75% and 59-60% in Year
529 2050 for dry bulk carriers and tankers, respectively.

530 The key limitations of the present modelling analysis, in our opinion, are the
531 uncertainties in the improvement of the future ship design and technological elements of
532 autonomous ships as well as the possibility of future route changes. We forecast the emission
533 changes at the ship-, port-, and voyage-level because they cover most of the ship's operation
534 and fuel consumption, therefore together produce a more comprehensive and realistic emission
535 outlook of autonomous shipping scenario. However, the transportation and supply chain might
536 evolve because of future inter-operation among digital ports and autonomous port operation.
537 Efforts should continue to examine these evolutionary trends in the future to achieve the
538 overarching environmental goals.

References

Abdelaal, M., Fränzle, M., Hahn, A.,2018. Nonlinear model predictive control for trajectory tracking and collision avoidance of underactuated vessels with disturbances. Ocean Eng, 160, 168-180.

Candeloro, M., Lekkas, A.M., Sørensen, A.J., 2017. A Voronoi-diagram-based dynamic path-planning system for underactuated marine vessels. Contr. Eng. Pract., 61, 41-54.

Contini, D., Gambaro, A., Donateo, A., Cescon, P., Cesari, D., Merico, E., Belosi, F., Citron, M., 2015. Inter annual trend of the primary contribution of ship emissions to $PM_{2.5}$ concentrations in Venice (Italy): Efficiency of emissions mitigation strategies. Atmos. Environ. 102, 183-190.

Dai, S., Wang, M., Wang C., 2016. Neural learning control of marine surface vessels with guaranteed transient tracking performance. IEEE Trans Indust Electron, 63 (3), 1717-1727.

DNV GL, 2015, Revolt report (2015-0170, Rev. 1), accessed 10 October 2020, https://www.dnvgl.com/technology-innovation/revolt/index.html.

Du, L., Goerlandt, F., Valdez Banda, O.A., Huang, Y., Wen, Y., Kujala, P., 2020. Improving stand-on ship's situational awareness by estimating the intention of the give-way ship. Ocean Eng., 201.

Faber, J., Nelissen, D., Hon, G., Wang, H.F., Tsimplis, M., 2012. Regulated slow steaming in maritime transport: an assessment of options, costs and benefits, accessed 11 February 2021, https://www.transportenvironment.org/sites/te/files/media/Slow%20steaming%20CE%20Delft%20final.pdf.

Fossen T.I., 2011. Handbook of marine craft hydrodynamics and motion control. Wiley, West Sussex, UK.

Garrido, S., Alvarez, D., Moreno, L.E., 2020. Marine applications of the fast marching method. Front. Robotics AI, 7.

Huang, Y., Chen, L., Chen, P., Negenborn, R.R., van Gelder, P.H.A.J.M., 2020. Ship collision avoidance methods: state-of-the-art. Saf. Sci., 121, 451-473.

IMO, 2021. Fourth IMO greenhouse gas study. London: International Maritime Organization.

Kongsberg Maritime, 2017, Yara and Kongsberg enter into partnership to build world first autonomous and zero emissions ship, accessed 8 October 2020, https://www.km.kongsberg.com/ks/web/nokbg0238.nsf/AllWeb/98A8C576AEFC85AFC125811A0037F6C4?OpenDocument.

KRISO, 2011. Korea- autonomous unmanned surface vessels (USV) for maritime survey and surveillance, accessed 8 February 2021, https://www.kriso.re.kr/eng/.

Liu, J.H., Duru, O., 2020. Bayesian probabilistic forecasting for ship emissions. Atmos. Environ. 231, 117540.

Liu, J.H., Duru, O., Law. A.W-K., 2021a. Assessment of atmospheric pollutant emissions with maritime energy strategies using Bayesian simulations and time series forecasting. Environ. Pollut. 270, 116068.

Liu, J.H., Law. A.W-K., Duru, O., 2021b. Abatement of atmospheric pollutant emissions with autonomous shipping in maritime transportation using Bayesian probabilistic forecasting. Atmos. Environ. 261, 118593.

Liu, Z.X., Zhang, Y.M., Yu, X., Yuan, C., 2016. Unmanned surface vehicles: an overview of developments and challenges. Annu. Rev. Contr., 41, 71-93.

Lloyd's Register, QinetiQ and University of Strathclyde, 2013, Global Marine Trends 2030, accessed 10 October 2020, https://www.lr.org/en-sg/insights/global-marine-trends-2030/.

MAN Diesel & Turbo, 2016. The flexible dual-fuel solution. Available online: https://mfame.guru/interview-rene-sejer-laursen-flexible-dual-fuel-solution/ (accessed on 28 January 2021).

Merico, E., Dinoi, A., Contini, D., 2019. Development of an integrated modelling-measurement system for near-real-time estimates of harbour activity impact to atmospheric pollution in coastal cities. Transp. Res. D. 73, 108-119.

MOL, 2017. MOL (Tokyo-Mitsui O.S.K. Lines, Ltd.) launches R&D on autonomous ocean transport system. Available online: https://www.mol.co.jp/en/pr/2017/17031.html (accessed on 28 January 2021).

MUNIN, 2016. Research in maritime autonomous systems project results and technology potentials. MUNIN.

NFAS, 2017, ASTAT - Autonomous Ship Transport at Trondheimsfjorden, accessed 8 November 2020, http://astat.autonomous-ship.org/.

Park, B.S., 2015. Adaptive formation control of underactuated autonomous underwater vehicles. Ocean Eng, 96, 1-7

Rødseth Ørnulf, J, 2013. Maritime unmanned navigation through intelligence in networks: The MUMIN project. Unmanned Ship 2013, 177–183.

Rolls-Royce, 2016a. Rolls-Royce Reveals Future Shore Control Centre. Available online: http://www.rolls-royce.com/media/press-releases/yr-2016/pr-2016-03-22-rr-reveals-future-shore-control-centre.aspx (accessed on 26 January 2021).

Rolls-Royce, 2016b. Remote and autonomous ships: the next steps. In: AAWA Adv. Auton. Waterborne Appl. 88.

Schonknecht, R, 1983. Ships and Shipping of Tomorrow. Cornell Maritime Pr.

Shen, H., Hashimoto, H., Matsuda, A., Taniguchi, Y., Terada, D., Guo, C., 2019. Automatic collision avoidance of multiple ships based on deep Q-learning. Appl. Ocean Res., 86, 268-288.

Singh, Y., Sharma, S., Sutton, R., Hatton, D., 2018. Towards use of Dijkstra algorithm for optimal navigation of an unmanned surface vehicle in a real-time marine environment with results from artificial potential field. TransNav, Int. J. Mar. Nav. Safety Sea Trans., 12 (1), 125-131.

SINTEF Ocean, 2020, The AEGIS (Advanced, Efficient and Green Intermodal Systems) project, accessed 8 November 2020, http://aegis.autonomous-ship.org/.

Skjetne, R., Smogeli, Y.N., Fossen, T.I., 2004. A nonlinear ship manoeuvring model: identification and adaptive control with experiments for a model ship. Model, Identif Control, 25 (1), 3-27.

Song, R., Liu, Y.C., Bucknall, R., 2017. A multi-layered fast marching method for unmanned surface vehicle path planning in a time-variant maritime environment. Ocean Eng., 129, 301-317.

Statheros, T., Howells, G., Mcdonald-maier, K., 2008. Autonomous ship collision avoidance navigation concepts, technologies and techniques. J. Navig., 61, 129-142.

Tam, C., Bucknall, R., Greig, A., 2009. Review of collision avoidance and path planning methods for ships in close range encounters. J. Navig., 62, 455-476.

Tao, L., Fairley, D., Kleeman, M.J., Harley, R.A., 2013. Effects of switching to lower sulphur marine fuel oil on air quality in the San Francisco Bay area. Environ. Sci. Technol. 47, 10171-10178.

Topaj, A.G., Tarovik, O.V., Bakharev, A.A., Kondratenko, A.A., 2019. Optimal ice routing of a ship with icebreaker assistance. Appl. Ocean Res., 86, 177-187.

Van Den Berg, J., Guy, S.J., Lin, M., Manocha, D., 2011. Reciprocal n-body collision avoidance. Springer Tr. Adv. Robot., 70, 3-19.

Xia, G., Han, Z., Zhao, B., Liu, C., Wang, X., 2019. Global path planning for unmanned surface vehicle based on improved quantum ant colony algorithm. Math. Probl Eng, 1-10.

Xue, Y., Clelland, D., Lee, B.S., Han, D., 2011. Automatic simulation of ship navigation. Ocean Eng., 38, 2290-2305.

Zhao, Z., He, W., Ge, S.S., 2014. Adaptive neural network control of a fully actuated marine surface vessel with multiple output constraints. IEEE Trans Control Syst Technol, 22 (4), 1536-1543.

Zhang, X., Wang, C., Liu, Y., Chen, X., 2019. Decision-making for the autonomous navigation of maritime autonomous surface ships based on scene division and deep reinforcement learning. Sensors, 19.

Zheng, H., Negenborn, R.R., Lodewijks, G., 2017. Closed-loop scheduling and control of waterborne agvs for energy-efficient inter terminal transport. Transport Res Part E: Logist Transport Rev, 105, 261-278.

Appendix

Table A.1 – Comparison of time series models (dry bulker carrier).

Sea Routes	*Method*	*Model*	*MAE*	*MASE*	*MAPE*	*MPE*	*RMSE*	*MDA*
Tubarao-Rotterdam	ARIMA	(0,1,1)	60.5	0.8	3.7	-0.6	80.5	0.7
	ETS	(M, M, N)	70.0	1.4	4.3	2.4	94.0	0.8
	Holt-Winters	additive	78.5	1.6	5.0	2.5	110.0	0.7
	NNAR	NNAR (12,1)	55.0	0.8	3.5	0.3	65.0	0.8
	Combined		12.0	0.8	8.7	-1.5	12.0	1.0
Tubarao-Kashima	ARIMA	(1,1,0) (0,0,1)12	60.5	0.8	5.0	2.5	80.5	1.2
	ETS	(M, N, M)	48.5	0.8	4.6	-1.5	55.0	0.8
	Holt-Winters	additive	70.0	1.2	6.7	-4.5	79.0	0.7
	NNAR	NNAR (1,1)	70.9	1.2	7.0	-5.2	79.9	0.9
	Combined		12.0	0.5	8.5	-2.0	14.5	0.9
Houston-Singapore	ARIMA	(1,1,1) (0,0,1)12	30.5	0.4	5.0	-3.0	35.0	0.8
	ETS	(M, N, M)	30.5	0.3	4.5	0.8	32.6	0.8
	Holt-Winters	additive	25.5	0.4	4.2	-1.2	33.4	0.8
	NNAR	NNAR (2,1)	25.5	0.3	5.6	-4.4	36.5	0.9
	Combined		16.5	0.2	4.4	-2.5	20.0	0.9

Table A.2 – Comparison of time series models (tanker).

Sea Routes	*Method*	*Model*	*MAE*	*MASE*	*MAPE*	*MPE*	*RMSE*	*MDA*
Ras Tanura-Qingdao	ARIMA	(0,0,0) 1,0,0)12	55.0	0.8	3.6	-0.8	73.4	0.9
	ETS	(A, N, N)	95.1	1.6	8.3	-9.1	104.5	0.8
	Holt-Winters	multiplicative	112.8	3.4	14.3	-15	119.5	0.8
	NNAR	NNAR (1,1)	46.5	0.9	3.6	0.5	55.5	0.8
	Combined		14.0	0.7	7.5	-2.3	15.5	0.8
Ras Tanura-Galveston	ARIMA	(1,0,0) (0,1,1)12	53.4	0.8	5.5	2.0	66.4	0.8
	ETS	(A, N, A)	47.9	0.5	3.9	-2.2	59.0	0.9
	Holt-Winters	additive	69.3	0.9	5.9	-3.8	77.5	0.8
	NNAR	NNAR (2,1,2)12	76.2	1.0	6.7	-4.8	76.8	0.9
	Combined		15.7	0.7	8.3	-2.4	14.4	0.9
Hedland-Tianjin	ARIMA	(1,1,0) (1,0,1)12	28.0	0.5	4.6	-2.7	40.3	0.8
	ETS	(M, A, N)	26.0	0.3	4.6	1.2	29.9	0.8
	Holt-Winters	additive	23.3	0.3	3.9	-0.8	26.4	0.8
	NNAR	NNAR (12,1)	35.5	0.6	6.5	-5.0	39.3	0.9
	Combined		17.6	0.2	3.2	-2.0	23.0	0.9

539

Table A.3 – Control Factor for NO_X and SO_X Emission Reduction.

Abatement Technique	*Fuel Sulphur S%*	*NO_X Reduction*	*SO_X Reduction in non-ECA Sulphur limit: 0.5%*
Exhaust gas recirculation		-35.0%	
Sea water scrubber	3.5%		-85.7%
	3.0%		-83.3%
	2.5%		-80.0%
	2.0%		-75.0%
	1.5%		-66.7%
	1.0%		-50.0%

Notes: Table A.3 lists the various abatement techniques and the emission reduction efficiency in the cases of NO_X and SO_X. The scrubber system is an emission abatement system equivalent to meet the low-Sulphur fuel requirement. To achieve that, the scrubber abatement efficiency depends on the Sulphur content in the fuel related to the Sulphur limit (Jalkanen et al., 2009; MAN Diesel & Turbo, 2015).

Table A.4 – Emission Factor (PM).

	Emission factor- PM								
	Main Engine			*Auxiliary Engine*			*Auxiliary Boiler*		
Load	VLSFO	LNG	Methanol	VLSFO	LNG	Methanol	VLSFO	LNG	Methanol
2%	2.59	0.22	0.00	2.62	0.22	2.62	1.46	0.22	1.46
3%	1.54	0.13	0.00	1.56	0.13	1.56	0.87	0.13	0.87
4%	1.10	0.09	0.00	1.11	0.09	1.11	0.62	0.09	0.62
5%	0.87	0.07	0.00	0.88	0.07	0.88	0.49	0.07	0.49
6%	0.72	0.06	0.00	0.73	0.06	0.73	0.41	0.06	0.41
7%	0.64	0.05	0.00	0.64	0.05	0.64	0.36	0.05	0.36
8%	0.57	0.05	0.00	0.58	0.05	0.58	0.32	0.05	0.32
9%	0.53	0.04	0.00	0.53	0.04	0.53	0.30	0.04	0.30
10%	0.49	0.04	0.00	0.50	0.04	0.50	0.28	0.04	0.28
11%	0.46	0.04	0.00	0.47	0.04	0.47	0.26	0.04	0.26
12%	0.44	0.04	0.00	0.45	0.04	0.45	0.25	0.04	0.25
13%	0.42	0.04	0.00	0.43	0.04	0.43	0.24	0.04	0.24
14%	0.41	0.03	0.00	0.41	0.03	0.41	0.23	0.03	0.23
15%	0.39	0.03	0.00	0.40	0.03	0.40	0.22	0.03	0.22
16%	0.38	0.03	0.00	0.39	0.03	0.39	0.22	0.03	0.22
17%	0.38	0.03	0.00	0.38	0.03	0.38	0.21	0.03	0.21
18%	0.37	0.03	0.00	0.37	0.03	0.37	0.21	0.03	0.21
19%	0.36	0.03	0.00	0.37	0.03	0.37	0.20	0.03	0.20
>20%	0.36	0.03	0.00	0.36	0.03	0.36	0.20	0.03	0.20

Notes: data on biofuel (biodiesel) emission factors are taken from Starcrest Consulting Group, LLC (2007); data on methanol emission factors are taken from Gilbert, et al., (2018).

Table A.5 – Emission Factor (SO_X).

	Emission factor- SO_X								
	Main Engine			*Auxiliary Engine*			*Auxiliary Boiler*		
Load	VLSFO	LNG	Methanol	VLSFO	LNG	Methanol	VLSFO	LNG	Methanol
2%	8.81	0.013	0.00	10.26	0.013	10.26	13.79	0.013	13.79
3%	5.56	0.008	0.00	6.47	0.008	6.47	8.70	0.008	8.70
4%	4.21	0.006	0.00	4.90	0.006	4.90	6.58	0.006	6.58
5%	3.48	0.005	0.00	4.06	0.005	4.06	5.45	0.005	5.45
6%	3.05	0.00	0.00	3.55	0.004	3.55	4.77	0.004	4.77
7%	2.76	0.004	0.00	3.21	0.004	3.21	4.32	0.004	4.32
8%	2.57	0.004	0.00	2.99	0.004	2.99	4.02	0.004	4.02
9%	2.42	0.003	0.00	2.81	0.003	2.81	3.78	0.003	3.78
10%	2.32	0.003	0.00	2.70	0.003	2.70	3.63	0.003	3.63
11%	2.23	0.003	0.00	2.59	0.003	2.59	3.48	0.003	3.48
12%	2.17	0.003	0.00	2.53	0.003	2.53	3.40	0.003	3.40
13%	2.11	0.003	0.00	2.46	0.003	2.46	3.31	0.003	3.31
14%	2.06	0.003	0.00	2.39	0.003	2.39	3.22	0.003	3.22
15%	2.02	0.003	0.00	2.35	0.003	2.35	3.16	0.003	3.16
16%	2.00	0.003	0.00	2.33	0.003	2.33	3.13	0.003	3.13
17%	1.96	0.003	0.00	2.28	0.003	2.28	3.07	0.003	3.07
18%	1.94	0.003	0.00	2.26	0.003	2.26	3.04	0.003	3.04
19%	1.92	0.003	0.00	2.24	0.003	2.24	3.01	0.003	3.01
>20%	1.90	0.003	0.00	2.22	0.003	2.22	2.98	0.003	2.98

Table A.6 – Emission Factor (NO_X, Year 2020).

	Emission factor- NO_X								
	Main Engine			*Auxiliary Engine*			*Auxiliary Boiler*		
Load	VLSFO	LNG	Methanol	VLSFO	LNG	Methanol	VLSFO	LNG	Methanol
2%	17.01	1.30	3.05	13.82	1.30	13.82	1.97	1.30	1.97
3%	17.01	1.30	3.05	13.82	1.30	13.82	1.97	1.30	1.97
4%	17.01	1.30	3.05	13.82	1.30	13.82	1.97	1.30	1.97
5%	17.01	1.30	3.05	13.82	1.30	13.82	1.97	1.30	1.97
6%	17.01	1.30	3.05	13.82	1.30	13.82	1.97	1.30	1.97
7%	17.01	1.30	3.05	13.82	1.30	13.82	1.97	1.30	1.97
8%	17.01	1.30	3.05	13.82	1.30	13.82	1.97	1.30	1.97
9%	17.01	1.30	3.05	13.82	1.30	13.82	1.97	1.30	1.97
10%	17.01	1.30	3.05	13.82	1.30	13.82	1.97	1.30	1.97
11%	17.01	1.30	3.05	13.82	1.30	13.82	1.97	1.30	1.97
12%	17.01	1.30	3.05	13.82	1.30	13.82	1.97	1.30	1.97
13%	17.01	1.30	3.05	13.82	1.30	13.82	1.97	1.30	1.97
14%	17.01	1.30	3.05	13.82	1.30	13.82	1.97	1.30	1.97
15%	17.01	1.30	3.05	13.82	1.30	13.82	1.97	1.30	1.97
16%	17.01	1.30	3.05	13.82	1.30	13.82	1.97	1.30	1.97
17%	17.01	1.30	3.05	13.82	1.30	13.82	1.97	1.30	1.97
18%	17.01	1.30	3.05	13.82	1.30	13.82	1.97	1.30	1.97
19%	17.01	1.30	3.05	13.82	1.30	13.82	1.97	1.30	1.97
>20%	17.01	1.30	3.05	13.82	1.30	13.82	1.97	1.30	1.97

Table A.7 – Emission Factor (NO_X from Year 2030-2050).

	Emission factor- NO_X								
	Main Engine			*Auxiliary Engine*			*Auxiliary Boiler*		
Load	VLSFO	LNG	Methanol	VLSFO	LNG	Methanol	VLSFO	LNG	Methanol
2%	17.01	1.30	3.05	13.82	1.30	13.82	1.97	1.30	1.97
3%	17.01	1.30	3.05	13.82	1.30	13.82	1.97	1.30	1.97
4%	17.01	1.30	3.05	13.82	1.30	13.82	1.97	1.30	1.97
5%	17.01	1.30	3.05	13.82	1.30	13.82	1.97	1.30	1.97
6%	17.01	1.30	3.05	13.82	1.30	13.82	1.97	1.30	1.97
7%	17.01	1.30	3.05	13.82	1.30	13.82	1.97	1.30	1.97
8%	17.01	1.30	3.05	13.82	1.30	13.82	1.97	1.30	1.97
9%	17.01	1.30	3.05	13.82	1.30	13.82	1.97	1.30	1.97
10%	17.01	1.30	3.05	13.82	1.30	13.82	1.97	1.30	1.97
11%	17.01	1.30	3.05	13.82	1.30	13.82	1.97	1.30	1.97
12%	17.01	1.30	3.05	13.82	1.30	13.82	1.97	1.30	1.97
13%	17.01	1.30	3.05	13.82	1.30	13.82	1.97	1.30	1.97
14%	17.01	1.30	3.05	13.82	1.30	13.82	1.97	1.30	1.97
15%	17.01	1.30	3.05	13.82	1.30	13.82	1.97	1.30	1.97
16%	17.01	1.30	3.05	13.82	1.30	13.82	1.97	1.30	1.97
17%	17.01	1.30	3.05	13.82	1.30	13.82	1.97	1.30	1.97
18%	17.01	1.30	3.05	13.82	1.30	13.82	1.97	1.30	1.97
19%	17.01	1.30	3.05	13.82	1.30	13.82	1.97	1.30	1.97
>20%	17.01	1.30	3.05	13.82	1.30	13.82	1.97	1.30	1.97

Table A.8 – Emission Factor (CO).

	Emission factor- CO								
	Main Engine			*Auxiliary Engine*			*Auxiliary Boiler*		
Load	VLSFO	LNG	Methanol	VLSFO	LNG	Methanol	VLSFO	LNG	Methanol
2%	13.58	12.61	0.00	10.67	12.61	10.67	1.94	12.61	1.94
3%	9.09	8.44	0.00	7.14	8.44	7.14	1.30	8.44	1.30
4%	6.80	6.32	0.00	5.35	6.32	5.35	0.97	6.32	0.97
5%	5.46	5.07	0.00	4.29	5.07	4.29	0.78	5.07	0.78
6%	4.56	4.24	0.00	3.59	4.24	3.59	0.65	4.24	0.65
7%	3.92	3.64	0.00	3.08	3.64	3.08	0.56	3.64	0.56
8%	3.43	3.19	0.00	2.70	3.19	2.70	0.49	3.19	0.49
9%	3.05	2.83	0.00	2.40	2.83	2.40	0.44	2.83	0.44
10%	2.76	2.56	0.00	2.17	2.56	2.17	0.39	2.56	0.39
11%	2.51	2.33	0.00	1.97	2.33	1.97	0.36	2.33	0.36
12%	2.30	2.13	0.00	1.80	2.13	1.80	0.33	2.13	0.33
13%	2.13	1.98	0.00	1.67	1.98	1.67	0.30	1.98	0.30
14%	1.97	1.83	0.00	1.55	1.83	1.55	0.28	1.83	0.28
15%	1.85	1.72	0.00	1.45	1.72	1.45	0.26	1.72	0.26
16%	1.74	1.61	0.00	1.36	1.61	1.36	0.25	1.61	0.25
17%	1.64	1.52	0.00	1.29	1.52	1.29	0.23	1.52	0.23
18%	1.55	1.44	0.00	1.22	1.44	1.22	0.22	1.44	0.22
19%	1.47	1.37	0.00	1.16	1.37	1.16	0.21	1.37	0.21
>20%	1.40	1.30	0.00	1.10	1.30	1.10	0.20	1.30	0.20

Table A.9 – Emission Factor (CO_2).

	Emission factor- CO_2								
	Main Engine			*Auxiliary Engine*			*Auxiliary Boiler*		
Load	VLSFO	LNG	Methanol	VLSFO	LNG	Methanol	VLSFO	LNG	Methanol
2%	590	457	522	686	457	686	922	457	922
3%	590	457	522	686	457	686	922	457	922
4%	590	457	522	686	457	686	922	457	922
5%	590	457	522	686	457	686	922	457	922
6%	590	457	522	686	457	686	922	457	922
7%	590	457	522	686	457	686	922	457	922
8%	590	457	522	686	457	686	922	457	922
9%	590	457	522	686	457	686	922	457	922
10%	590	457	522	686	457	686	922	457	922
11%	590	457	522	686	457	686	922	457	922
12%	590	457	522	686	457	686	922	457	922
13%	590	457	522	686	457	686	922	457	922
14%	590	457	522	686	457	686	922	457	922
15%	590	457	522	686	457	686	922	457	922
16%	590	457	522	686	457	686	922	457	922
17%	590	457	522	686	457	686	922	457	922
18%	590	457	522	686	457	686	922	457	922
19%	590	457	522	686	457	686	922	457	922
>20%	590	457	522	686	457	686	922	457	922

Table A.10 – Emission Factor (CH_4).

	Emission factor- CH_4								
	Main Engine			*Auxiliary Engine*			*Auxiliary Boiler*		
Load	VLSFO	LNG	Methanol	VLSFO	LNG	Methanol	VLSFO	LNG	Methanol
2%	0.25	180.03	0.00	0.17	180.03	0.17	0.04	180.03	0.04
3%	0.14	99.28	0.00	0.09	99.28	0.09	0.02	99.28	0.02
4%	0.09	65.54	0.00	0.06	65.54	0.06	0.02	65.54	0.02
5%	0.07	47.69	0.00	0.04	47.69	0.04	0.01	47.69	0.01
6%	0.05	36.98	0.00	0.03	36.98	0.03	0.01	36.98	0.01
7%	0.04	29.92	0.00	0.03	29.92	0.03	0.01	29.92	0.01
8%	0.04	25.08	0.00	0.02	25.08	0.02	0.01	25.08	0.01
9%	0.03	21.42	0.00	0.02	21.42	0.02	0.01	21.42	0.01
10%	0.03	18.53	0.00	0.02	18.53	0.02	0.00	18.53	0.00
11%	0.02	16.66	0.00	0.02	16.66	0.02	0.00	16.66	0.00
12%	0.02	14.96	0.00	0.01	14.96	0.01	0.00	14.96	0.00
13%	0.02	13.60	0.00	0.01	13.60	0.01	0.00	13.60	0.00
14%	0.02	12.50	0.00	0.01	12.50	0.01	0.00	12.50	0.00
15%	0.02	11.56	0.00	0.01	11.56	0.01	0.00	11.56	0.00
16%	0.02	10.71	0.00	0.01	10.71	0.01	0.00	10.71	0.00
17%	0.01	10.03	0.00	0.01	10.03	0.01	0.00	10.03	0.00
18%	0.01	9.44	0.00	0.01	9.44	0.01	0.00	9.44	0.00
19%	0.01	8.93	0.00	0.01	8.93	0.01	0.00	8.93	0.00
>20%	0.01	8.50	0.00	0.01	8.50	0.01	0.00	8.50	0.00